International Journal of Nanomedicine

Dovepress
open access to scientific and medical research

Open Access Full Text Article

ORIGINAL RESEARCH

Fe_3O_4/Au magnetic nanoparticle amplification strategies for ultrasensitive electrochemical immunoassay of alfa-fetoprotein

This article was published in the following Dove Press journal:
International Journal of Nanomedicine
8 December 2011
Number of times this article has been viewed

Ning Gan[1]*
Haijuan Jin[1]*
Tianhua Li[1]
Lei Zheng[2]

[1]The State Key Laboratory Base of Novel Functional Materials and Preparation Science, Faculty of Material Science and Chemical Engineering, Ningbo University, Ningbo, [2]Department of Laboratory Medicine, Nanfang Hospital, Southern Medical University, Guangzhou, People's Republic of China

*Both authors contributed equally to this work

Background: The purpose of this study was to devise a novel electrochemical immunosensor for ultrasensitive detection of alfa-fetoprotein based on Fe_3O_4/Au nanoparticles as a carrier using a multienzyme amplification strategy.

Methods and results: Greatly enhanced sensitivity was achieved using bioconjugates containing horseradish peroxidase (HRP) and a secondary antibody (Ab_2) linked to Fe_3O_4/Au nanoparticles (Fe_3O_4/Au-HRP-Ab_2) at a high HRP/Ab_2 ratio. After a sandwich immunoreaction, the Fe_3O_4/Au-HRP-Ab_2 captured on the electrode surface produced an amplified electrocatalytic response by reduction of enzymatically oxidized hydroquinone in the presence of hydrogen peroxide. The high content of HRP in the Fe_3O_4/Au-HRP-Ab_2 could greatly amplify the electrochemical signal. Under optimal conditions, the reduction current increased with increasing alfa-fetoprotein concentration in the sample, and exhibited a dynamic range of 0.005–10 ng/mL with a detection limit of 3 pg/mL.

Conclusion: The amplified immunoassay developed in this work shows good precision, acceptable stability, and reproducibility, and can be used for detection of alfa-fetoprotein in real samples, so provides a potential alternative tool for detection of protein in the laboratory. Furthermore, this immunosensor could be regenerated by simply using an external magnetic field.

Keywords: Fe_3O_4/Au nanoparticles, alfa-fetoprotein, sandwich immunoassay, electrochemical immunosensor

Introduction

It is well known that alfa-fetoprotein (AFP), an oncofetal glycoprotein with a molecular weight of approximately 70,000 Da, is a tumor marker that occurs mainly in hepatocellular carcinoma, yolk sac tumors, and the serum of patients with other malignant tumors.[1–3] The average concentration of AFP in healthy human serum is <20 ng/mL, and serum AFP levels often increase in a number of disease states.[4] Therefore, detection of trace amounts of AFP is of great importance. Thus far, various immunosensors and immunoassays based on different measurement principles have been reported for determination of AFP, including enzyme-linked immunosorbent assay (ELISA),[5] electrochemiluninescence,[6,7] chemiluminescence,[8,9] surface plasmon resonance[10,11] and quartz crystal microbalance.[12,13] ELISA is the most widely used immunoassay method in the laboratory. However, concentrations of tumor-related proteins are very low in the early stages of cancer, and are beyond the detection limit of ELISA. Moreover, their lengthy analysis requires highly skilled personnel, specially equipped laboratories, and expensive reagents.[14] Thus, new methods that can rapidly and conveniently monitor tumor-related proteins are highly desirable. Electrochemical immunosensors,

Correspondence: Ning Gan
Faculty of Material Science and Chemical Engineering, Ningbo University, Ningbo 315211, People's Republic of China
Tel +86 574 8760 9933
Fax +86 574 8760 0734
Email ganning@nbu.edu.cn

Lei Zheng
Department of Laboratory Medicine, Nanfang Hospital, Southern Medical University, Guangzhou 510515, People's Republic of China
Tel +86 20 6164 2147
Fax +86 20 6278 7681
Email nfyyzl@163.com

based on specificity of antigen–antibody interactions with electrochemical transducers, have attracted considerable interest because of their intrinsic advantages, such as low cost, high sensitivity, simple instrumentation, and excellent compatibility with miniaturization technologies.[15] Therefore, different electrochemical immunosensors, particularly amperometric immunosensors, have been developed and applied extensively for the determination of AFP.[16–18]

In order to meet the increasing demand for early and ultrasensitive detection of tumor markers, three primary signal amplification strategies using nanomaterials have been developed.[19] The first method involves the use of metal and semiconductor nanoparticles directly as electroactive labels to amplify the electrochemical detection of proteins.[20,21] The second method uses nanoparticles as carriers for loading a large amount of electroactive species to amplify the detection signal.[22,23] The third method is the most extensively employed, and uses enzyme-functionalized nanoparticles as labels. Enhanced sensitivity was achieved by loading a large amount of enzyme towards an individual sandwich immunological reaction event. Recently, various types of nanomaterials have been used as carriers for loading enzymes and antibodies to enhance sensitivity, including gold nanoparticles,[24] irregularly shaped gold nanoparticles,[25] nanosilica particles,[26] carbon nanoparticles,[27,28] carbon nanotubes,[29] and graphene oxide.[30] For example, Chen et al have proposed a highly sensitive electrochemical immunosensor using irregular gold nanoparticles as carriers of horseradish peroxidase (HRP)-anti-AFP for signal amplification.[25] Similarly, Lin et al have reported use of graphene oxide, a novel tracer, to label HRP and the antibody, and developed an ultrasensitive immunoassay method for detection of phosphorylated p53 (S392).[30]

Recently, hybrid nanomaterials consisting of two or more different nanoscale functionalities have attracted much attention due to their novel combined properties and multiple potential applications.[31] Immunomagnetic beads in particular are widely used in enrichment and separation of particular proteins in biology samples.[32–34] Among them, magnetic composite Fe_3O_4/Au nanoparticles have attracted particular attention, owing to the combined functions of Fe_3O_4 and gold. Fe_3O_4 nanoparticles have a typical superparamagnetic nature, and provide a convenient means for separation, isolation, and purification of biological samples via an external magnetic field when the functional reagents are attached onto the surface of the particles.[35,36] Their unique structural, electronic, and optical properties make gold nanoparticles very attractive for several applications in biotechnology.[37–39] Further, gold nanoparticles can provide a natural environment for bimolecular immobilization and facilitate electron transfer of biosensors because of their large surface area, interesting electrochemical properties, and good biocompatibility.[40–42] Therefore, magnetic composite Fe_3O_4/Au nanoparticles have had more and more applications in areas such as immunoassays, protein immobilization, cell purification, and magnetically controlled transport of anticancer drugs.[43–46]

Our present work focuses on enzyme-enriched, magnetic functionalized nanoparticles in signal amplification and separation for ultrasensitive detection of AFP. Magnetic composite Fe_3O_4/Au nanoparticles were synthesized by assembling gold nanoparticles on SH-modified Fe_3O_4 and using them as nanocarriers for immobilization of HRP and a secondary antibody (Ab_2). Greatly amplified sensitivity is achieved using bioconjugates featuring HRP and Ab_2 linked to Fe_3O_4/Au at a high HRP/Ab_2 ratio for replacement of singly labeled secondary antibodies. A modified glass carbon electrode with porous nanostructured gold film was used to attach the primary antibody (Ab_1). The analytical procedure consists of immunoreaction of the antigen (AFP) with Ab_1, followed by binding of Fe_3O_4/Au-HRP-Ab_2. Electrochemical detection was performed in the presence of H_2O_2 and hydroquinone (Figure 1). The results demonstrated that an immunosensor based on this amplification strategy has a good dynamic range from 0.005 to 10 ng/mL and a low detection limit of 3 pg/mL for AFP. This simple, cost-effective, and sensitive immunosensor could find wide potential application in clinical analysis.

Materials and methods

Reagents and materials

Monoclonal mouse antihuman AFP and AFP test kits were obtained from Zhengzhou Biocell Biochem Company (Zhengzhou, China). Fe_3O_4 (20 nm in diameter), 3-mercaptopropyltriethoxysilane (3-MPTES) and HRP (EC 1.11.1.7, RZ $>$ 3.0, A $>$ 250 U/mg) were purchased from Sigma-Aldrich, St Louis, MO. Hydrogen tetrachloroaurate (III) tetrahydrate ($HAuCl_4 \cdot 4H_2O$), trisodium citrate, hydroquinone, H_2O_2, and bovine serum albumin were obtained from Sinopharm Group Chemical Reagent Company Ltd (Shanghai, China). All reagents used were of analytical reagent grade, and all solutions were prepared with double deionized water. Phosphate-buffered solutions 0.1 M of various pH values were prepared by mixing stock solutions of NaH_2PO_4 and Na_2HPO_4, and then the pH was adjusted with 0.1 M NaOH and H_3PO_4.

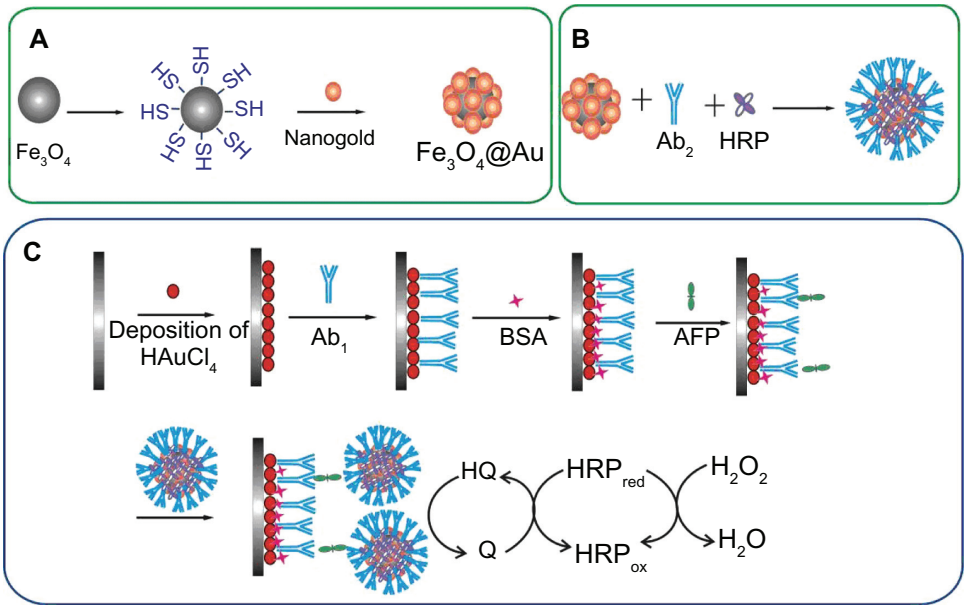

Figure 1 Schematic representation of the preparation of (**A**) Fe_3O_4/Au, (**B**) Fe_3O_4/Au-HRP-Ab_2, and (**C**) immunosensor.
Abbreviations: AFP, alfa-fetoprotein; BSA, bovine serum albumin; HRP, horseradish peroxidase; Ab_2, secondary antibody.

Apparatus

Cyclic voltammetry measurements were performed using an electrochemical analyzer CHI 660 (Shanghai Chenhua Instrumental Corp, China) connected to a personal computer. A three-compartment electrochemical cell contained a platinum wire auxiliary electrode, a saturated calomel reference electrode, and a modified glass carbon electrode (GCE, 2 mm in diameter) as working electrode. The sizes of the nanoparticles were estimated from transmission electron microscopy (H-7650, Hitachi Instruments, Tokyo, Japan). The surface topographic features and composition of variously modified electrodes were characterized using scanning electron microscopy coupled with energy dispersive spectroscopy (SEM-EDS, S3400N Hitachi). The x-ray powder diffraction images were obtained using a Bruker D8 Advance diffractometer (Bruker, Karlsruhe, Germany). Ultraviolet-visible spectra were recorded using a TU-1901 spectrophotometer (Purkinje General Instrument Co, Beijing, China). The x-ray photoelectron spectra were taken using an AXIS UltraDLD spectrometer (Shimadzu Co, Tokyo, Japan). Vibrating sample magnetometry (Lake Shore 7410) was used to perform magnetic measurements on the dried samples to evaluate the magnetic properties of the nanoparticles.

Preparation of Fe_3O_4/Au nanoparticles

Figure 1A shows the procedure used to prepare the Fe_3O_4/Au. First, gold nanoparticles was prepared using the Frens method.[47] In brief, 0.01 wt% $HAuCl_4$ (100 mL) was boiled with vigorous stirring in a flask. Trisodium citrate 1 wt% solution (2.5 mL) was added quickly to the boiling solution, resulting in a color change from pale yellow to dark red, indicating formation of gold nanoparticles. The solution was maintained for 10 minutes at boiling temperature.

Fe_3O_4/Au nanoparticles were obtained by self-assembling gold nanoparticles onto the surface of SH-modified Fe_3O_4 according to the literature with modification.[48] Fe_3O_4 nanoparticles are commercially available. Experimentally, Fe_3O_4 0.2 g was dispersed in 50% ethanol 90 mL by ultrasound, and then 3-MPTES 300 µL and ammonium hydroxide 500 µL were added dropwise. The mixture was stirred at 60°C for 6 hours under a nitrogen atmosphere. Uncoated Fe_3O_4 was deleted by means of washing with 0.1 M HCl (six times, for four hours each). The deposit was separated by a magnetic stirrer, which was rinsed three times with double deionized water and then ethanol to give SH-modified Fe_3O_4. Following that, the gold nanoparticles were added to the SH-modified Fe_3O_4, and shaken slightly for 4 hours at room temperature to make the gold assemble on the surface of the formed nanoparticles. After magnetic separation, the Fe_3O_4/Au obtained were rinsed with double deionized water and suspended in 10 mL water.

Preparation of Fe_3O_4/Au-HRP-Ab_2 conjugates

Figure 1B shows the procedure used to prepare the Fe_3O_4/Au-HRP-Ab_2 bioconjugate. Initially, 1.0 mL of a 1.0 mg/mL Fe_3O_4/Au nanoparticle suspension was adjusted to pH 8.2

using Na_2CO_3. Thereafter, 200 µL of HRP at 1 mg/mL and 200 µL of Ab_2 at 10 µg/mL were added to the dispersion, and the mixture was stirred overnight at 4°C. After magnetic separation and washing three times, the resulting mixture was redispersed in 1.0 mL of pH 7.4 phosphate-buffered solution containing 1% bovine serum albumin and stored at 4°C.

Fabrication of the immunosensor

The procedure followed to prepare the proposed immunosensor is schematized in Figure 1C. The GCE was polished with 0.3 µm and 0.05 µm alumina, followed by successive sonication in distilled water and ethanol for 5 minutes and dried in air. A porous nanostructure gold film was then deposited at a voltage of –0.5 V for 50 seconds on the clean GCE that was immersed in 5 mL 0.08 M $HAuCl_4$ solution containing 0.004 M lead acetate. After thorough washing with water, the electrode was immediately followed by incubation with 20 µL 0.5 mg/mL Ab_1 for one hour. After washing with 0.05% Tween-20 and phosphate-buffered solution, Ab_1/Au/GCE was incubated in 3% bovine serum albumin and phosphate-buffered solution at 37°C for one hour to block excess active groups and nonspecific binding sites on the surface. The electrode was then washed with 0.05% Tween-20 and phosphate-buffered solution before use.

Immunoassay procedure for detection of AFP

A sandwich immunoassay was used for determination of AFP. The immunosensor, Ab_1/Au/GCE, was incubated with 20 µL of a different concentration of standard AFP antigen for 30 minutes at 25°C, followed by washing with 0.05% Tween-20 and phosphate-buffered solution. Next, the electrode was incubated with 20 µL of Fe_3O_4/Au-HRP-Ab_2 for 30 minutes at 25°C, followed by washing with 0.05% Tween-20 and phosphate-buffered solution to remove the nonspecific adsorption of conjugate. Electrochemical detection was performed in 5 mL of pH 6.5 phosphate-buffered solution containing 2 mM hydroquinone and 5 mM H_2O_2, and from –0.6 to 0.6 V (versus saturated calomel reference electrode) with a scan rate of 100 mV/second.

Results and discussion

Characterization of Fe_3O_4/Au-HRP-Ab_2 conjugation

In this work, Fe_3O_4/Au was as an excellent carrier for HRP and Ab_2 because of its good biocompatibility, large surface area, and superparamagnetic properties. Transmission electron microscope images provide more detailed morphological information on the prepared nanoparticles (Figure 2). They demonstrated that both Fe_3O_4 and Fe_3O_4/Au nanoparticles were spherical in structure, monodispersed, and of appropriate size. The average diameter of the Fe_3O_4/Au nanoparticles was about 40 nm (Figure 2C). Upon deposition of gold onto the Fe_3O_4 nanoparticles, the diameter of the particles increased by about 20 nm, demonstrating that the thickness of the gold was about 10 nm.

Figure 3A compares the x-ray powder diffraction pattern for the Fe_3O_4 nanoparticles and Fe_3O_4/Au nanoparticles. In Figure 3A (curve a), the diffraction peak positions at $2\theta = 30.0°$, 35.3°, 42.6°, 53.4°, and 62.5° can be attributed to the (220), (311), (400), (422), (511), and (440) planes of Fe_3O_4 in a cubic phase (space group Fd3 m), respectively. In Figure 3A (curve b), the diffraction peak positions at $2\theta = 38.1°$, 44.2°, 64.5°, 77.5°, and 81.6° can be attributed to the (111), (200), (220), (311), and (222) planes, respectively. Other peaks can be attributed to Fe_3O_4, and the simultaneous observation of both Fe_3O_4 and gold peaks verified successful assembly of Fe_3O_4/Au nanoparticles.

The surface composition of elements such as iron and gold in the Fe_3O_4/Au nanoparticles were determined by x-ray

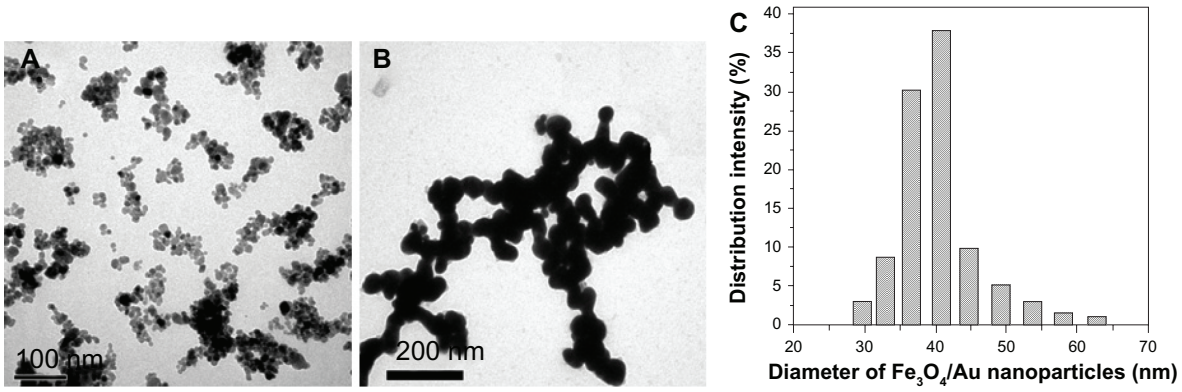

Figure 2 Transmission electron microscopic images of (**A**) Fe_3O_4 and (**B**) Fe_3O_4/Au. Diameter distribution of (**C**) Fe_3O_4/Au nanoparticles.

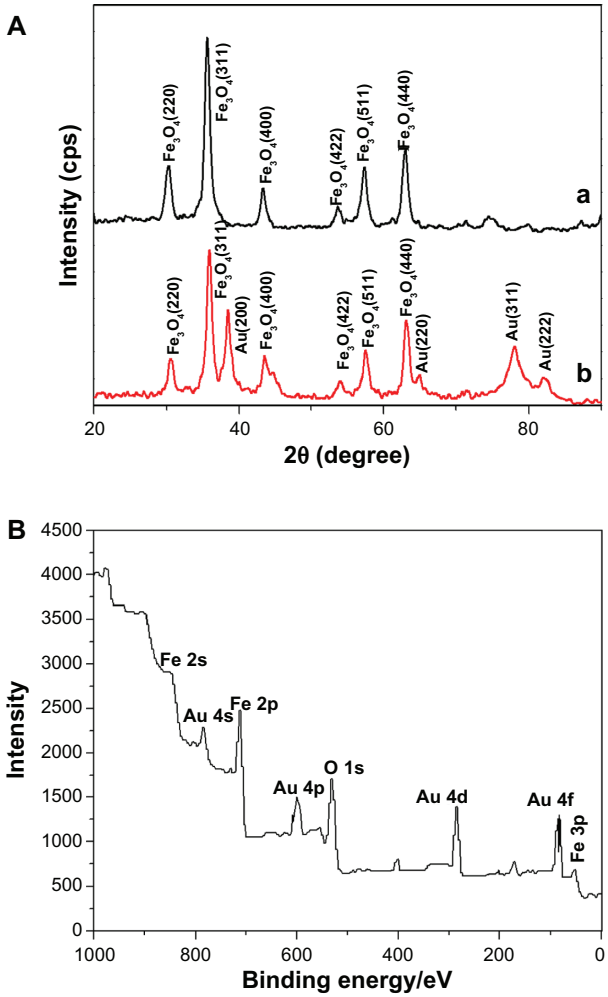

Figure 3 (**A**) X-ray powder diffraction patterns for (**a**) Fe_3O_4 nanoparticles and (**b**) Fe_3O_4/Au nanoparticles. (**B**) X-ray photoelectron spectra binding-energy spectra for a sample of Fe_3O_4/Au.

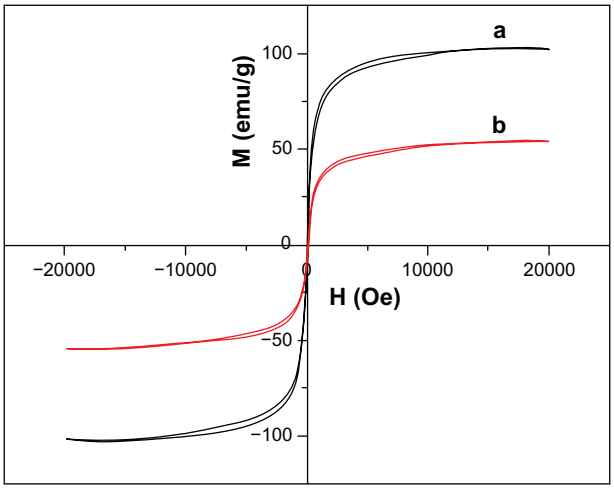

Figure 4 Magnetization hysteresis for (**a**) Fe_3O_4 and (**b**) Fe_3O_4/Au nanoparticles recorded at room temperature.

photoelectron spectra as shown in Figure 3B. Figure 3B shows gold peaks including Au 4s, Au 4p, Au 4d, and Au 4f appearing on the surface of the Fe_3O_4 nanoparticles. The Au 4f appearing at 80–90 eV can be assigned to the Au^0. The Fe_3O_4 showed Fe 2p at 700–720 eV. The x-ray photoelectron spectra result was in agreement with a report by Cui et al indicating that gold had been successfully assembled on the surface of the magnetic Fe_3O_4 nanoparticles.[48]

The magnetic properties of the nanoparticles are illustrated in Figure 4. It can be seen that a small coercivity or remanence existed around room temperature, indicating the Fe_3O_4 and Fe_3O_4/Au have superparamagnetic properties. As a result, the Fe_3O_4/Au could be isolated from solution by an adscititious magnet. It can also be seen that the saturation magnetization for Fe_3O_4/Au is much smaller than that for Fe_3O_4. The saturation magnetization values were 76.8 emu/g and 54.9 emu/g for Fe_3O_4 and Fe_3O_4/Au nanoparticles, respectively.

The saturation magnetization value of the magnetic nanoparticles declined after coating with a layer of gold. This lower saturation magnetization value is due to the presence of nonmagnetic gold.

The Fe_3O_4/Au-HRP-Ab_2 obtained was characterized by ultraviolet-visible spectroscopy and, as shown in Figure 5, the Fe_3O_4 nanoparticles did not show any obvious absorbance peaks in ultraviolet-visible spectroscopy (curve a). However, the Fe_3O_4/Au nanoparticles showed a clear absorption band containing a maximum centered at 540 nm (curve c). This band showed a red shift in comparison with pure gold nanoparticles (curve b, 520 nm). This finding suggests that a combination of Fe_3O_4 nanoparticles and gold nanocomposites leads to a red shift of resonant wavelength. After Ab_2 and HRP were conjugated onto the Fe_3O_4/Au, two absorption peaks around 280 nm and 404 nm were observed (curve f), which can be ascribed to the typical absorption of Ab_2 (curve d) and HRP (curve e).

SEM-EDS characterization of gold nanoparticles modified electrode with direct electroposition

SEM-EDS were used to investigate the successful fabrication of the immunosensor. Figure 6A shows the energy dispersive spectroscopy analysis of Au/GCE showing Au-M (2.0 keV), Au-Lα (9.7 keV), and Au-Lβ (11.4 keV), which indicates successful electrodeposition of gold on the GCE. Furthermore, scanning electron microscopy was used to investigate the Au/GCE before and after modification with Ab_1. As shown in Figure 6B, many small porous gold nanoparticles were obtained on the Au/GCE. Obviously, the

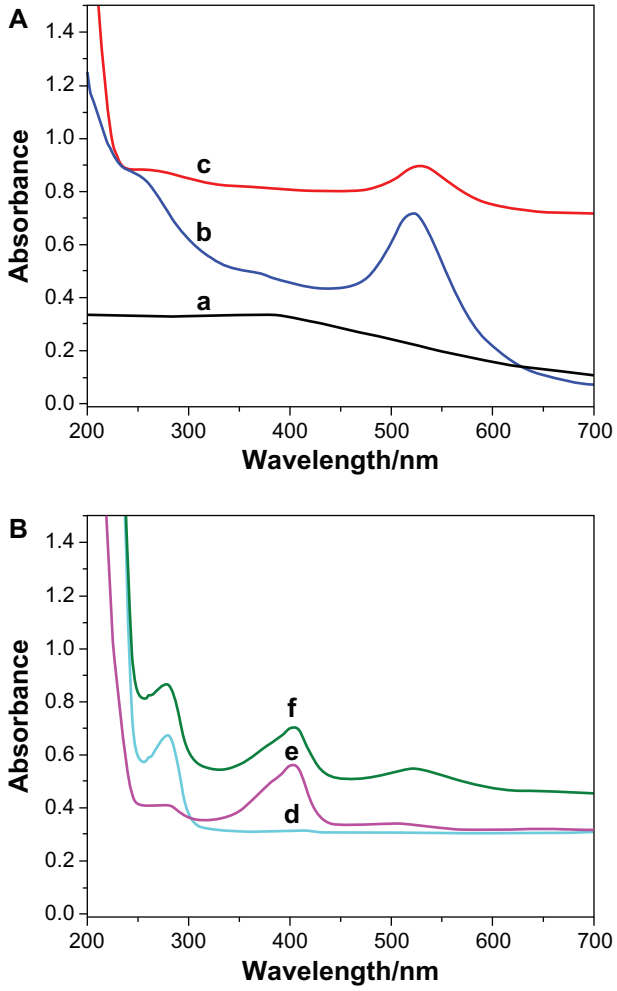

Figure 5 Ultraviolet-visible spectra for (**a**) Fe_3O_4, (**b**) Au, (**c**) Fe_3O_4/Au, (**d**) Ab_2, (**e**) HRP, and (**f**) Fe_3O_4/Au-HRP-Ab_2.
Abbreviations: HRP, horseradish peroxidase; Ab_2, secondary antibody.

porous gold film-modified electrode had a larger surface compared with the ordinary glassy carbon electrode, which could provide a larger surface area for the immobilization of Ab_1. Upon immobilization of Ab_1, obvious aggregation of the trapped biomolecules could be observed on the surface (Figure 6C), indicating successful immobilization of Ab_1.

Electrochemical characterization of the immunosensor

As shown in Figure 7, the cyclic voltammograms of Ab_1/Au/GCE did not show any detectable signal in pH 6.5 phosphate-buffered solution (curve a). Upon adding 2 mM hydroquinone and 5 mM H_2O_2 to the phosphate-buffered solution, Ab_1/Au/GCE exhibited a pair of stable and well defined redox peaks at −145 mV and 345 mV (curve b), corresponding to the electrochemical redox response of hydroquinone on the electrode surface. When incubating the immunosensor with 5 ng/mL AFP antigen, no obvious change in signal was observed.

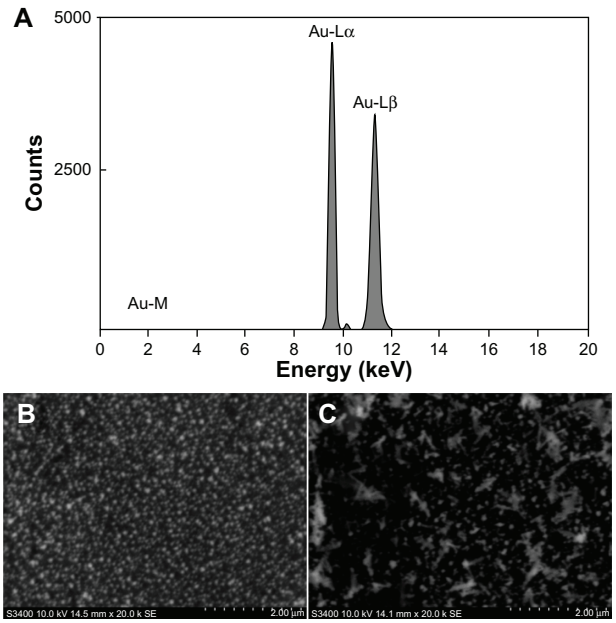

Figure 6 (**A**) Energy dispersive spectroscopy pattern of Au/GCE electrode. Scanning electron microscopic images of (**B**) Au/GCE and (**C**) Ab_1/Au/GCE.
Abbreviation: GCE, glass carbon electrode.

However, after incubation with Fe_3O_4/Au-HRP-Ab_2, the resulting sandwich immunocomplex displayed an obvious increase in electrocatalytic reduction current (curve c) because of the introduction of HRP onto the electrode surface by the immunoreaction.

Comparison of detection antibodies with various labels

To investigate further the effect of the synthesized Fe_3O_4/Au on the sensitivity of the electrochemical immunosensors,

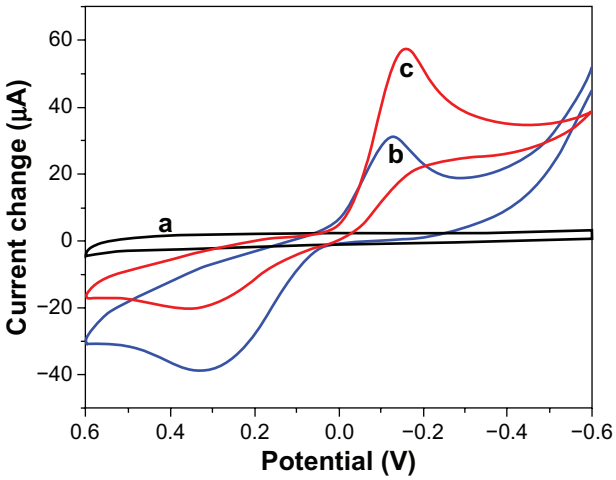

Figure 7 Cyclic voltammograms obtained at (**a**) Ab_1/Au/GCE in pH 6.5 phosphate-buffered solution, (**b**) Ab_1/Au/GCE, (**c**) Fe_3O_4/Au-HRP-Ab_2/AFP/Ab_1/Au/GCE, in pH 6.5 phosphate-buffered solution containing 2 mM hydroquinone and 5 mM H_2O_2.
Abbreviations: HRP, horseradish peroxidase; GCE, glass carbon electrode.

three types of detection antibodies were used, ie, HRP-anti-Ab_2, Au-HRP-Ab_2, and Fe_3O_4/Au-HRP-Ab_2 (Figure 8). As shown in Figure 8A–C, upon addition of H_2O_2 to the substrate solution, an obvious catalytic characteristic appeared, with a distinct increase in the reduction current and a decrease in the oxidation current. The catalytic current

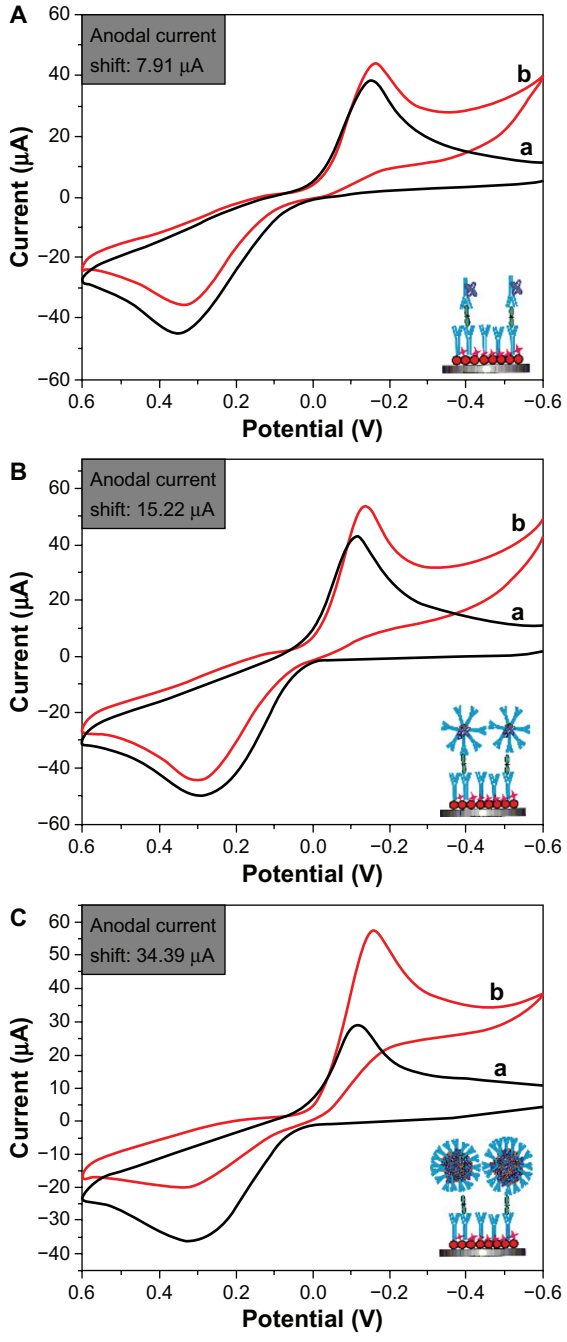

Figure 8 Cyclic voltammograms of the electrochemical sandwich immunosensors toward 5 ng/mL alfa-fetoprotein in the absence (**A**) and presence (**B**) of 5 mM H_2O_2 in an electrolytic cell in phosphate-buffered solution containing 2 mM hydroquinone by using various detection antibodies (**a**) HRP-anti-Ab_2, (**b**) Au-HRP-Ab_2, and (**C**) Fe_3O_4/Au-HRP-Ab_2.
Abbreviations: HRP, horseradish peroxidase; Ab_2, secondary antibody.

is mainly due to the labeled HRP toward the reduction of H_2O_2 with the help of hydroquinone as an electron mediator. As shown in Figure 8, we found that the electrochemical immunosensor exhibited a larger current shift using Au-HRP-Ab_2 (Figure 8B) as the detection antibody than when using HRP-anti-Ab_2 (Figure 8A). The reason for this might be that the gold nanoparticles with a high surface-to-volume ratio and good biocompatibility can load more HRP and Ab_2. Moreover, gold nanoparticles have good conductivity, which can enhance enzyme activity.[49] More significantly, the electrochemical responses could be improved by using Fe_3O_4/Au-HRP-Ab_2 (Figure 8C) rather than Au-HRP-Ab_2 (Figure 8B). A possible reason is that Fe_3O_4 can allow more room for attachment of gold nanoparticles, which indirectly increases the amount of bound Ab_2 and HRP. When one antibody molecule on the surface of Fe_3O_4/Au-HRP-Ab_2 is reacted with the corresponding antigen, other HRP molecules can enter and participate in the electrochemical reaction. At the same time, Fe_3O_4/Au can enhance the electron transfer rate between the enzyme and the electrode.[50,51]

Optimization of immunoassay conditions

Because of the coimmobilization of enzymes and antibodies on the Fe_3O_4/Au nanocarrier, the ratio of HRP and Ab_2 is the most important factor in the response signal. As shown in Figure 9A, one can see that the electrocatalytic current increases with an increasing ratio of HRP/Ab_2, and the maximum response is achieved at a ratio of 100:1. An increase in the HRP/Ab_2 ratio could increase the total amount of HRP loaded per Fe_3O_4/Au nanocarrier, which would be expected to increase the response amplification for this sandwich immunoassay. However, reducing the amount of Ab_2 in the immunoassay may decrease the efficiency of the immune reaction to the AFP antigen captured at the electrode surface, which may result in a decreased response. Therefore, an HRP/Ab_2 ratio of 100:1 was selected as the optimal condition in which to prepare the Fe_3O_4/Au-HRP-Ab_2 conjugate. To determine the amount of active HRP in the Fe_3O_4/Au-HRP-Ab_2 conjugate dispersion, the mixture was reacted with the TMB substrate for HRP. The reaction product was read at 650 nm. These results were compared with a standard curve constructed using pure HRP as part of an enzyme activity experiment. The concentration of active HRP in the Fe_3O_4/Au-HRP-Ab_2 conjugate dispersion was determined to be 7.14 μg/mL.

The pH of the detection solution is an important parameter because the acidity of the solution is greatly affected by the activity of immobilized proteins. The effect of pH

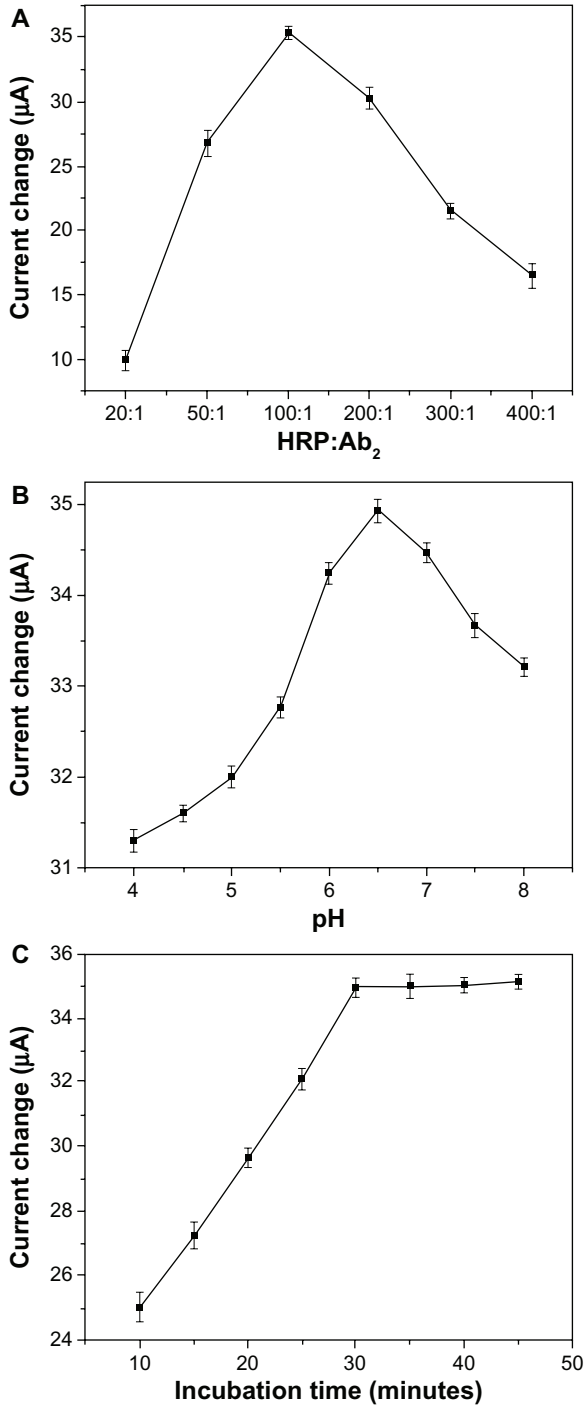

Figure 9 Effects of (**A**) HRP/Ab_2 ratio, (**B**) pH of phosphate-buffered solution, and (**C**) incubation time on electrochemical responses. A 1 ng/mL AFP concentration was used during the incubation process.
Abbreviations: Ab_2, secondary antibody; AFP, alfa-fetoprotein; HRP, horseradish peroxidase.

of the solution on the amperometric response for AFP is shown in Figure 9B. The current response was increased by increments in pH from 4.0 to 6.5 and then decreased when pH exceeded 6.5. Therefore, a 0.1 M solution of pH 6.5 was selected as the optimum solution for AFP detection.

The temperature and time taken for the antigen-antibody interaction to occur greatly influenced the sensitivity of the sandwich-type immunoassay developed. Considering the practical applications of the proposed system in clinical immunoassays, all experiments were carried out at room temperature (25°C ± 1.0°C). Under this condition, the effect of various incubation times (10–45 minutes) on the immunosensor current was investigated at 1 mg/mL of AFP. As shown in Figure 9C, the reduction current increased with increasing incubation time and tended to level off after 30 minutes, indicating optimal formation of the sandwich-type immunocomplexes. A longer incubation time could not improve the response. Therefore, 30 minutes of incubation time was used for the detection of AFP in this study.

Analytical performance

The cyclic voltammograms of the immunosensor was investigated by assaying various AFP standards using Fe_3O_4/Au-HRP-Ab_2 as trace labels and H_2O_2 as the enzyme substrate. The reduction current increased with incremental AFP concentration in the incubation solution. As shown by curve a in Figure 10, the increase in reduction current was proportional to AFP concentration in the range of 0.005–10 ng/mL; the linear regression equation is $\Delta i_p(\mu A) = 13.3 \times \log C_{AFP}$ (ng/mL) + 42.2 with a detection limit of 3 pg/mL ($R^2 = 0.988$). For comparison, we also investigated the analytical performance of the immunosensor using Au-HRP-Ab_2 and HRP-anti-AFP as detection antibodies, respectively. The regression equations, linear ranges, and detection limits are as follows:

Using Au-HRP-Ab_2 (Figure 9 curve b):

$$\Delta i_p(\mu A) = 5.88 \times \log C_{AFP} \text{ (ng/mL)} + 13.0,$$
$$R^2 = 0.990,\ 0.01–10 \text{ ng/mL},\ 6 \text{ pg/mL AFP} \quad \text{(i)}$$

Using HRP-anti-AFP (Figure 9 curve c):

$$\Delta i_p(\mu A) = 3.51 \times \log C_{AFP} \text{ (ng/mL)} + 3.88,$$
$$R^2 = 0.962,\ 1.0–10 \text{ ng/mL},\ 0.6 \text{ ng/mL AFP} \quad \text{(ii)}$$

These results suggest that Fe_3O_4/Au could greatly improve the sensitivity and work range of the immunosensor. Although the threshold of human serum AFP is 10 ng/mL, actual serum samples should be diluted during the clinical diagnostic process, so the concentrations detected are usually <10 ng/mL. Small volume samples are preferable. Thus, the sensitivity of this immunoassay was adequate for practical application.

Regeneration of immunosensors is of great interest to immunoanalysts. Traditional regeneration of the immunosensor usually requires a different regeneration solution, such as an

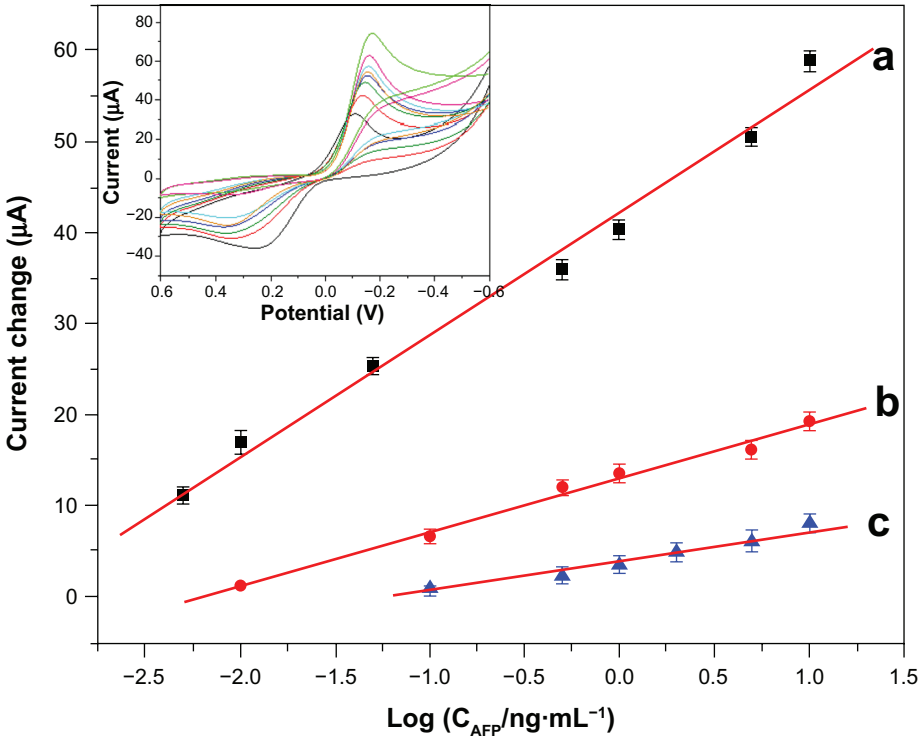

Figure 10 Calibration curves for the electrochemical immunosensor towards the AFP standard using various detection antibodies: (**a**) Fe_3O_4/Au-HRP-Ab_2, (**b**) Au-HRP-Ab_2, and (**c**) HRP-anti-AFP (inset: cyclic voltammograms of the immunosensor using Fe_3O_4/Au-HRP-Ab_2 towards AFP standard with various concentrations from bottom to top: 0, 0.005, 0.01, 0.05, 0.5, 1, 5 and10 ng/mL in pH 6.5 phosphate-buffered solution containing 5 mM H_2O_2 and 2 mM hydroquinone).
Abbreviations: Ab_2, secondary antibody; AFP, alfa-fetoprotein; HRP, horseradish peroxidase.

acid, alkali, or electrolyte solution at a high concentration to break the linkage between the antigen and antibody. In the present work, the immunosensor could be regenerated by simply using an external magnetic field to remove the Fe_3O_4/Au-HRP-Ab_2-bonded antigen. Experimental results indicated that the immunosensor could retain 90.7% of the initial current response for 18 applications once regenerated.

Immunosensor specificity, reproducibility, and stability

Specificity is an important feature of the immunosensor. To investigate this, the immunosensor was incubated with 1 ng/mL AFP containing a different interference substance, such as carcinoma antigen 125, carcinoembryonic antigen, human IgG, prostate-specific antigen, and bovine serum albumin. No remarkable change of currents was observed in comparison with the results obtained in the presence of AFP only, indicating good selectivity of the proposed AFP immunosensor.

The reproducibility of the proposed immunosensor was evaluated by intra-assay and interassay coefficients of variation. The intra-assay precision of the analytical method was evaluated by analyzing one immunosensor for six replicate determinations. Coefficients of variation for the intra-assay were 3.6% and 4.7% at 0.1 ng/mL and 1.0 ng/mL AFP, respectively. Similarly, the interassay coefficients of variation for six immunosensor determinations were 3.9% and 5.5% at 0.1 ng/mL and 1.0 ng/mL AFP, respectively. These results demonstrate the acceptable reproducibility and precision of the proposed immunosensor.

We also examined the stability of the developed immunosensor. When not in use, the immunosensor could be stored in pH 7.0 phosphate-buffered solution at 4°C for at least 3 weeks without any obvious signal change. Moreover, the immunosensor retained 89.4% of its initial response after a storage period of 4 weeks. The slow decrease in current response may be attributed to gradual deactivation of biomolecules immobilized on the nanoparticle surface.

Application of the immunosensor in human serum

The electrochemical immunosensor was further validated by assaying six serum specimens gifted from the Nanfang Medical Hospital, China. The serum was prepared by collecting whole blood, leaving it undisturbed for 15–30 minutes at room temperature to clot, and then removing the clot by centrifugation at 1000–2000 rpm for 10 minutes in a refrigerated centrifuge, and collecting the supernatant serum. Table 1 describes the correlation between the partial results obtained by the

Table 1 Comparison of serum AFP levels determined using two methods

Serum samples	1	2	3	4	5	6
Immunosensor (ng/mL)[a]	20.9	12.1	53.9	96.3	33.6	3.2
ELISA[a]	19.6	11.5	51.5	93.5	31.9	–[b]
Relative deviation (%)[c]	6.6	5.2	4.7	3.0	5.3	

Notes: [a]Average value of five successive determinations; [b]not detected; [c]relative deviation was calculated by comparing results obtained using the present method with reference values obtained by the commercial ELISA method.
Abbreviations: AFP, alfa-fetoprotein; ELISA, enzyme-linked immunosorbent assay.

proposed immunosensor and the ELISA method, indicating no significant difference between the two methods, ie, the proposed immunosensor could be used for satisfactory clinical determination of AFP levels in human serum.

Conclusion

We have successfully designed a multienzyme labeling Fe_3O_4/Au strategy as part of a signal amplification procedure and demonstrated its use in the ultrasensitive, selective, and accurate quantification of AFP by electrochemical immunoassay. Highlights of the developed immunoassay are: Fe_3O_4/Au as the enzyme-loading carrier can load many enzyme molecules on each Fe_3O_4/Au nanoparticle, thus enhancing the sensitivity of the immunosensor; using Fe_3O_4/Au as signal enhancers favors rapid separation and purification of the signal antibody on an external magnetic field; after each detection, the immunosensor can be easily regenerated by applying an external magnetic field. The proposed immunosensor has high sensitivity, good reproducibility, stability, and accuracy. We anticipate that this method can be extended for determination of other proteins and have promising potential in clinical applications.

Acknowledgments

This work was supported by the National Natural Science Foundation of China (20805024, 81072336), the Natural Science Foundation of Ningbo (2011A610018, 2011A610006), the Social Development Project of Ningbo (2011C50038), and the KC Wong Magna Fund in Ningbo University, Science and Technology Planning Project of Guangdong Province (2010A030300006, 2008A050200006).

Disclosure

The authors report no conflicts of interest in this work.

References

1. Gitlin D, Perricelli A, Gitlin GM. Synthesis of α-fetoprotein by liver, yolk sac, and gastrointestinal tract of the human conceptus. *Cancer Res*. 1972;32:979–982.
2. Won YS, Lee SW. Targeted retardation of hepatocarcinoma cells by specific replacement of alpha-fetoprotein RNA. *J Biotechnol*. 2007;129:614–619.
3. Badera D, Riskina A, Vafsia O, et al. Alpha-fetoprotein in the early neonatal period – a large study and review of the literature. *Clin Chim Acta*. 2004;349:15–23.
4. Tatsuta M, Yamamura H, Lishi H, Kasugai H, Okuda S. Value of serum alpha-fetoprotein and ferritin in the diagnosis of hepatocellular carcinoma. *Oncology*. 1986;43:306–310.
5. Jia CP, Zhong XQ, Hua B, et al. Nano-ELISA for highly sensitive protein detection. *Biosens Bioelectron*. 2009;24:2836–2841.
6. Wang HY, Sun DY, Tan ZA, Gong W, Wang L. Electrochemiluminescence immunosensor for α-fetoprotein using $Ru(bpy)_3^{2+}$-encapsulated liposome as labels. *Colloids Surf B Interfaces*. 2011;84:515–519.
7. Yuan SR, Yuan R, Chai YQ, et al. Sandwich-type electrochemiluminescence immunosensor based on Ru-silica@Au composite nanoparticles labeled anti-AFP. *Talanta*. 2010;82:1468–1471.
8. Fu ZF, Hao C, Fei XQ, Ju HX. Flow-injection chemiluminescent immunoassay for α-fetoprotein based on epoxysilane modified glass microbeads. *J Immunol Methods*. 2006;312:61–67.
9. Bi S, Yan YM, Yang XY, Zhang SS. Gold nanolabels for new enhanced chemiluminescence immunoassay of alpha-fetoprotein based on magnetic beads. *Chem Eur J*. 2009;15:4704–4709.
10. Homola J. Surface plasmon resonance sensors for detection of chemical and biological species. *Chem Rev*. 2008;108:462–493.
11. Teramura YJ, Iwata H. Label-free immunosensing for a-fetoprotein in human plasma using surface plasmon resonance. *Anal Biochem*. 2007;365:201–207.
12. Luo Y, Chen M, Wen QJ, et al. Rapid and simultaneous quantification of 4 urinary proteins by piezoelectric quartz crystal microbalance immunosensor array. *Clin Chem*. 2006;52:2273–2280.
13. Chou SF, Hsu WL, Hwang JM, Chen CY. Determination of α-fetoprotein in human serum by a quartz crystal microbalance-based immunosensor. *Clin Chem*. 2002;48:913–918.
14. Zhang YX, Zhang ZJ, Yang F. A sensitive immunoassay for determination of hepatitis B surface antigen and antibody in human serum using capillary electrophoresis with chemiluminescence detection. *J Chromatogr B*. 2007;857:100–107.
15. Wang J, Ibanez A, Chatrathi MP, Escarpa A. Electrochemical enzyme immunoassays on microchip platforms. *Anal Chem*. 2001;73:5323–5327.
16. Lin JH, He CY, Zhang LJ, Zhang SS. Sensitive amperometric immunosensor for a-fetoprotein based on carbon nanotube/gold nanoparticle doped chitosan film. *Anal Biochem*. 2009;384: 130–135.
17. Wei Q, Mao KX, Wu D, et al. A novel label-free electrochemical immunosensor based on graphene and thionine nanocomposite. *Sensor Actutators B*. 2010;149:314–318.
18. Su BL, Tang DP, Li QF, Tang J, Chen GN. Gold-silver-graphene hybrid nanosheets-based sensors for sensitive amperometric immunoassay of alpha-fetoprotein using nanogold-enclosed titania nanoparticles as labels. *Anal Chim Acta*. 2011;692:116–124.
19. Wu YF, Chen CL, Liu SQ. Enzyme-functionalized silica nanoparticles as sensitive labels in biosensing. *Anal Chem*. 2009;81:1600–1607.
20. Cui RJ, Pan HC, Zhu JJ, Chen HY. Versatile immunosensor using CdTe quantum dots as electrochemical and fluorescent labels. *Anal Chem*. 2007;79:8494–8501.
21. Ho JA, Lin YC, Wang LS, Hwang KC, Chou PT. Carbon nanoparticle-enhanced immunoelectrochemical detection for protein tumor marker with cadmium sulfide biotracers. *Anal Chem*. 2009;81: 1340–1346.
22. Cui RJ, Liu C, Shen JM, Gao D, Zhu JJ, Chen HY. Gold nanoparticle-colloidal carbon nanosphere hybrid material: preparation, characterization, and application for an amplified electrochemical immunoassay. *Adv Funct Mater*. 2008;18:2197–2204.
23. Jie GF, Huang HP, Sun XL, Zhu JJ. Electrochemiluminescence of CdSe quantum dots for immunosensing of human prealbumin. *Biosens Bioelectron*. 2008;23:1896–1899.

24. Cui RJ, Huang HP, Yin ZZ, Gao D, Zhu JJ. Horseradish peroxidase-functionalized gold nanoparticle label for amplified immunoanalysis based on gold nanoparticles/carbon nanotubes hybrids modified biosensor, *Biosens Bioelectron*. 2008;23:1666–1673.
25. Tang J, Su BL, Tang DP, Chen GN. Conductive carbon nanoparticles-based electrochemical immunosensor with enhanced sensitivity for α-fetoprotein using irregular-shaped gold nanoparticles-labeled enzyme-linked antibodies as signal improvement. *Biosens Bioelectron*. 2010;25:2657–2662.
26. Tang DP, Su BL, Tang J, Ren JJ, Chen GN. Nanoparticle-based sandwich electrochemical immunoassay for carbohydrate antigen 125 with signal enhancement using enzyme-coated nanometer-sized enzyme-doped silica beads. *Anal Chem*. 2010;82:1527–1534.
27. Tang J, Huang JX, Su BL, Chen HF, Tang DP. Sandwich-type conductometric immunoassay of alpha-fetoprotein in human serum using carbon nanoparticles as labels. *Biochem Eng J*. 2011;53:223–228.
28. Du D, Zou ZX, Shin YS, et al. Functionalized graphene oxide as a nanocarrier in a multienzyme labeling amplification strategy for ultrasensitive electrochemical immunoassay of phosphorylated p53 (S392). *Anal Chem*. 2010;82:2989–2995.
29. Malhotra R, Patel V, Vaque JP, Gutkind JS, Rusling JF. Ultrasensitive electrochemical immunosensor for oral cancer biomarker IL-6 using carbon nanotube forest electrodes and multilabel amplification. *Anal Chem*. 2010;82:3118–3123.
30. Du D, Wang LM, Shao YY, Wang J, Engelhard MH, Lin YH. Sensitive immunosensor for cancer biomarker based on dual signal amplification strategy of graphene sheets and multienzyme functionalized carbon nanospheres. *Anal Chem*. 2011;83:746–752.
31. Sanchez C, Julian B, Belleville P, Popall M. Applications of hybrid organic-inorganic nanocomposites. *J Mater Chem*. 2005;15:3559–3592.
32. Tang DP, Yuan R, Chai YQ. Ultrasensitive electrochemical immunosensor for clinical immunoassay using thionine-doped magnetic gold nanospheres as labels and horseradish peroxidase as enhancer. *Anal Chem*. 2008;80:1582–1588.
33. Xu LX, Kim MJ, Kim KD, Choa YH, Kim HT. Surface modified Fe_3O_4 nanoparticles as a protein delivery vehicle. *Colloids Surf., A*. 2009;350:8–12.
34. Park ME, Chang JH. High throughput human DNA purification with aminosilanes tailored silica-coated magnetic nanoparticles. *Mater Sci Eng., C*. 2007;27:1232–1235.
35. Kim DK, Zhang Y, Voit W, et al. Superparamagnetic iron oxide nanoparticles for bio-medical applications. *Scripta Mater*. 2001;44:1713–1717.
36. Pankhurst QA, Connolly J, Jones SK, Dobson J. Applications of magnetic nanoparticles in biomedicine. *J Phys D: Appl Phys*. 2003;36:167–181.
37. Nasr MB, Goode DP, Nguyen N, et al. Quantum optical coherence tomography of a biological sample. *Opt Commun*. 2009;282:1154–1159.
38. Skrabalak SE, Chen JY, Sun YG, et al. Gold nanocages: synthesis, properties, and applications. *Acc Chem Res*. 2008;41:1587–1595.
39. Skrabalak SE, Chen JY, Au L, Lu XM, Li XD, Xia YN. Gold nanocages for biomedical applications. *Adv Mater.* 2007;19:3177–3184.
40. Ambrosi A, Castaneda MT, Killard AJ, Smyth MR, Alegret S, Merkoci A. Double-codified gold nanolabels for enhanced immunoanalysis. *Anal Chem*. 2007;79:5232–5240.
41. Alfredo M, Christian SE, Freitas BD, Fernandez AG, Marisa MC, Arben M. Rapid identification and quantification of tumor cells using an electrocatalytic method based on gold nanoparticles. *Anal Chem*. 2009;81:10268–10274.
42. Ambrosi A, Airo F, Merkoc A. Enhanced gold nanoparticle based ELISA for a breast cancer biomarker. *Anal Chem*. 2010;82:1151–1156.
43. Qiu JD, Xiong M, Liang RP, Peng HP, Liu F. Facile preparation of magnetic core/shell Fe_3O_4@Au nanoparticle/myoglobin biofilm for direct electrochemistry. *Biosens Bioelectron*. 2009;24:2649–2653.
44. Park HY, Schadt MJ, Wang LY, et al. Fabrication of magnetic core@shell Fe oxide@Au nanoparticles for interfacial bioactivity and bio-separation. *Langmuir*. 2007;23:9050–9056.
45. Liu HL, Sonn CH, Wu JH, Lee KM, Kim YK. Synthesis of streptavidin-FITC-conjugated core–shell Fe_3O_4-Au nanocrystals and their application for the purification of $CD4^+$ lymphocytes. *Biomaterials*. 2008;29:4003–4010.
46. Son SJ, Reichel J, He B, Schuchman M, Lee SB. Magnetic nanotubes for magnetic-field-assisted bioseparation, biointeraction, and drug delivery. *J Am Chem Soc*. 2005;127:7316–7317.
47. Frens G. Controlled nucleation for the regulation of the particle size in monodisperse gold suspensions. *Nature Phys. Sci*. 1973;241:20–22.
48. Cui YL, Zhang LY, Su J, et al. Preparation and mechanism of Fe_3O_4/Au core/shell super-paramagnetic microspheres. *Sci Ser B*. 2001;44:404–410.
49. Xu J, Shang FJ, Luong JHT, Razeeb KM, Glennon JD. Direct electrochemistry of horseradish peroxidase immobilized on a monolayer modified nanowire array electrode. *Biosens Bioelectron*. 2010;25:1313–1318.
50. Kouassi GK, Irudayaraj J, McCarty G. Examination of cholesterol oxidase attachment to magnetic nanoparticles. *J Nanobiotechnology*. 2005;3:1–9.
51. Thandavan K, Gandhi S, Sethuraman S, et al. A novel nanostructured iron oxide-gold bioelectrode for hydrogen peroxide sensing. *Nanotechnology*. 2011;22:5505–5515.